Angewandte
International Edition Chemie

DOI: 10.1002/anie.201001110

Ferromagnetic Materials

Combined Magnetic Susceptibility Measurements and ^{57}Fe Mössbauer Spectroscopy on a Ferromagnetic {$Fe^{III}_4Dy_4$} Ring[**]

*Dirk Schray, Ghulam Abbas, Yanhua Lan, Valeriu Mereacre, Alexander Sundt, Jan Dreiser, Oliver Waldmann, George E. Kostakis, Christopher E. Anson, and Annie K. Powell**

In memory of Ian J. Hewitt

In the search for smaller and more effective magnetic devices, attention has recently turned to Fe^{III}–4f heterometallic complexes because these combine the readily and cheaply available highly paramagnetic high-spin Fe^{III} ion with highly anisotropic 4f ions, and some of the complexes have been shown to act as single-molecule magnets (SMMs).[1] In the majority of the SMM systems described to date, the dominant magnetic interactions tend to be antiferromagnetic in nature, but there can be little doubt that the design of novel ferromagnetic molecular materials is of great interest in terms of producing high-spin molecular systems.[2] In such a context, the prediction and characterization of the ferromagnetic nature of the interaction in the molecular complexes based on transition metal ions have become fairly well established.[3,4] However, understanding the nature of interactions in systems involving lanthanide ions is much more challenging. In fact, until relatively recently, there were few magnetic studies on molecular materials containing lanthanide and transition metal ions because of the weak interactions present and the added complications introduced by the orbital contribution of lanthanide ions.[5] Herein we describe how, by using a combination of magnetic susceptibility measurements and Mössbauer spectroscopy, we have been able to shed light on the nature of the magnetic interactions in the first ferromagnetically coupled coordination cluster containing Dy^{III} and Fe^{III} ions.

The reaction of $FeCl_3$, $DyCl_3{\cdot}6H_2O$, triethanolamine ($teaH_3$), and NaN_3 in a 2:1:3:2 molar ratio in MeCN/CH_3OH gave a red solution from which orange crystals of the compound $[Fe_4Dy_4(teaH)_8(N_3)_8(H_2O)]{\cdot}4(CH_3CN)(H_2O)$ (**1**) formed over three days. Complex **1** (Figure 1) crystallizes in the monoclinic space group $P2_1/n$. The structure of **1** is based on a ring-like $[Fe_4Dy_4]^{24+}$ core, with alternating Fe^{III} and Dy^{III} centers, which slightly but significantly deviates from planarity towards a saddle-like geometry. Three adjacent metal atoms, Fe(2), Dy(2), and Fe(3), show slight disorder, with the minor (12.3%) component corresponding to a lesser distortion from planarity; no attempt was made to resolve the

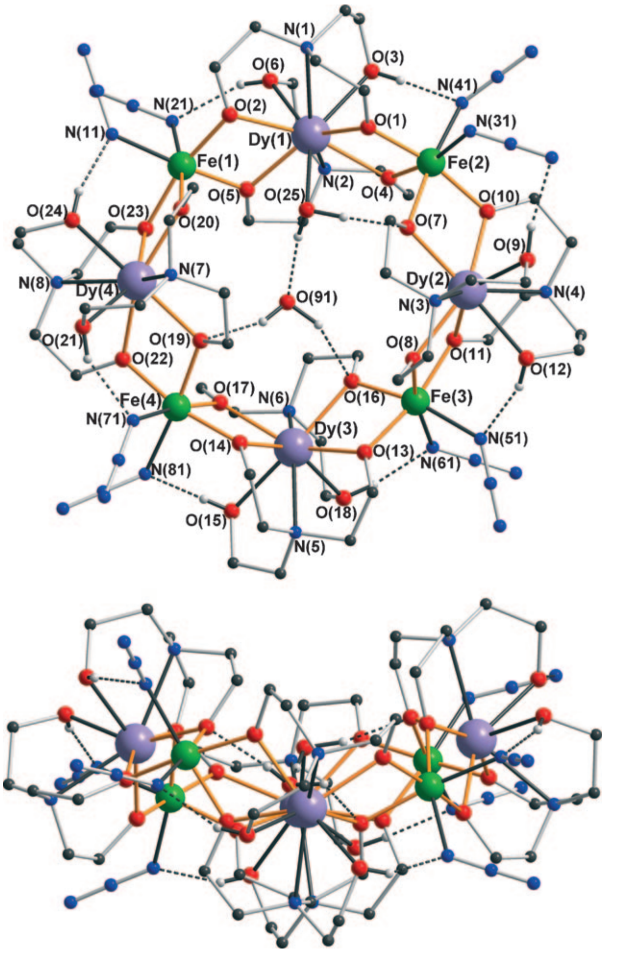

Figure 1. Molecular structure of **1**, showing hydrogen bonding (dotted) and the saddle-like distortion from planarity of the core. Lattice MeCN molecules, disordered atoms, and methylene H atoms are omitted for clarity.

---

[*] D. Schray, Dr. G. Abbas, Dr. Y. Lan, Dr. V. Mereacre, Dr. C. E. Anson, Prof. Dr. A. K. Powell
Institute of Inorganic Chemistry
Karlsruhe Institute of Technology
Engesserstrasse 15, 76128 Karlsruhe (Germany)
Fax: (+49) 721-608-8142
E-mail: annie.powell@kit.edu

Dr. G. E. Kostakis
Institute of Nanotechnology
Karlsruhe Institute of Technology
Postfach 3640, 76021 Karlsruhe (Germany)

A. Sundt, Dr. J. Dreiser, Prof. O. Waldmann
Physikalisches Institut, Universität Freiburg
Hermann-Herder-Strasse 3, 79104 Freiburg (Germany)

[**] We thank the DFG Center for Functional Nanostructures for financial support.

Supporting information for this article is available on the WWW under http://dx.doi.org/10.1002/anie.201001110.

ligand atoms of the minor component. Each Dy^{III} cation is chelated by two doubly-deprotonated (teaH)$^{2-}$ ligands, with the four deprotonated oxygen atoms forming pairs of μ-alkoxo bridges (shown as orange lines in Figure 1) to the two adjacent Fe^{III} ions in the ring. The coordination shells of the four iron centers are each completed by two monodentate azide ligands to give octahedral *cis*-N_2O_4 environments.

The protonated alcohol arms of the (teaH)$^{2-}$ ligands coordinate in a terminal mode to their respective Dy centers, with each forming a hydrogen bond to a nitrogen atom of an azide ligand. For Dy(2), Dy(3), and Dy(4), these alcohol oxygen atoms complete the distorted square-antiprismatic N_2O_6 coordination environments. However, Dy(1) is additionally coordinated by an aqua ligand, O(25), resulting in a capped square-antiprismatic N_2O_7 environment and the unusually high coordination number of nine for this Dy^{III} center. Atom O(25) forms hydrogen bonds to a bridging alkoxo oxygen, O(7), and a water molecule, O(91), situated close to the centroid of the Dy_4Fe_4 ring. Atom O(91) itself forms two further hydrogen bonds to the alkoxo oxygen atoms O(16) and O(19), and these interactions serve to stabilize the ring structure.

All of the alkoxo bridges have similar geometries, with Fe-O-Dy angles in the range 105.60(15)–109.79(15)°, and Fe–O bonds of 1.954(3)–2.078(4) Å and Dy–O 2.265–2.376(3) Å. The Fe⋯Dy distances are in the range 3.4572(7)–3.5120(10) Å. As expected, the Dy–O distances to the protonated alcohol oxygen atoms (2.401(3)–2.483(3) Å) are longer as is the distance to the water oxygen (2.444(4) Å). The Dy–N distances are in the range 2.574(4)–2.634(5) Å and the Fe–N distances are between 2.088(5) and 2.208(5) Å.

Direct current (DC) magnetic susceptibility data for **1** were collected in the 1.8–300 K temperature range under a field of 0.1 T (Figure 2a). The value for the product χT at 300 K is 72.4 cm^3 K mol^{-1}, which is in agreement with the expected value of 74.18 cm^3 K mol^{-1} for four HS Fe^{3+} with $g = 2$, $S = 5/2$, $C = 4.375$ cm^3 K mol^{-1} and four Dy^{3+} ions with $g = 4/3$, $S = 5/2$, $L = 5$, $J = 15/2$, $C = 14.17$ cm^3 K mol^{-1}. On lowering the temperature, the χT product stays almost constant until around 60 K, increases continuously to reach a maximum value of 161.2 cm^3 K mol^{-1} at 3 K, and then rapidly falls to 146.1 cm^3 K mol^{-1} at 1.8 K. This type of magnetic behavior indicates the presence of dominant ferromagnetic interactions within this compound that are strong enough to not be overwhelmed by any thermal depopulation of the Dy^{III} excited states. The final decrease of χT is likely to result from magnetic anisotropy and/or antiferromagnetic intercluster interactions, although no obvious exchange pathways exist between the molecules.

The field dependence of the magnetization curves at low temperatures shows a rapid increase at low fields, which then increases with only a slight slope and thus without clear saturation up to 7 T, where it reaches 38.6 μ_B (Figure 2b). The presence of ferromagnetic interactions is also supported by the rapid increase of the magnetization below 5 K at low fields. The high-field behavior of the magnetization also suggests the presence of significant magnetic anisotropy. Furthermore, when plotting M versus H/T at different fields (Supporting Information, Figure S1), the curves are not superposed onto a single master-curve, giving a further indication of the presence of these effects.

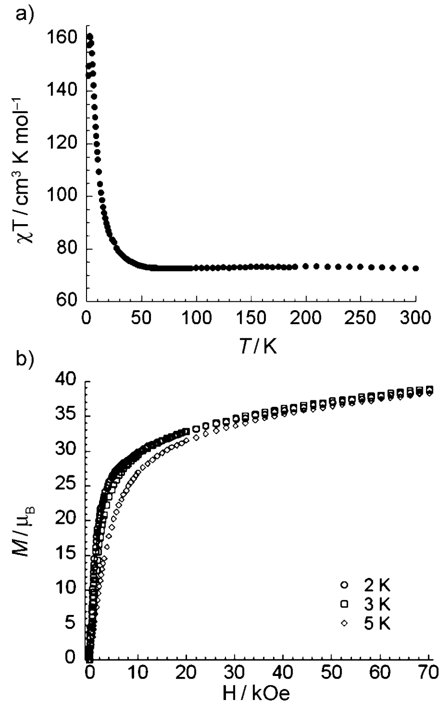

Figure 2. a) Plot of $\chi_M T$ versus T under an applied DC field of 0.1 T for **1**. b) Plot of M versus H at the indicated temperatures.

The alternating current (AC) magnetic susceptibilities were studied as a function of temperature and frequency. The data (Supporting Information, Figures S2, S3) reveal that compound **1** possesses strong frequency-dependent in-phase and out-of-phase signals below 4 K, indicating slow relaxation of the magnetization. The maximum of the out-of-phase signal was observed at 2.8 K at a frequency of 1500 Hz. The relaxation time deduced from the AC data (both frequency-dependent and temperature-dependent) follows an activated Arrhenius law behavior with an energy gap Δ of 30.5 K and a pre-exponential factor τ_0 of 2.0×10^{-9} s (Supporting Information, Figure S4). The frequency dependence of the AC susceptibility in an applied DC field was also measured at 1.8 K (Supporting Information, Figure S5) to determine whether the relaxation rate would decrease as a result of the presence of a quantum tunneling relaxation pathway. With increasing field, the relaxation rate $1/\tau$ remains essentially constant below 1000 Oe, indicating that for **1**, at least above 1.8 K, there is no quantum tunneling of the magnetization.

Figure 3 shows the normalized magnetization M/M_s of a polycrystalline sample of **1** versus applied magnetic field at two different temperatures and at a constant sweep rate of 0.46 T s^{-1}. At 1.4 K, the compound exhibits a clear hysteretic behavior, which disappeared at 6.8 K. The hysteresis depends strongly on the field sweep rate (Supporting Information, Figure S6). At 1.4 K, coercive field values could be extracted (90 mT at 0.46 T s^{-1}, 40 mT at 0.1 T s^{-1}, and 10 mT at

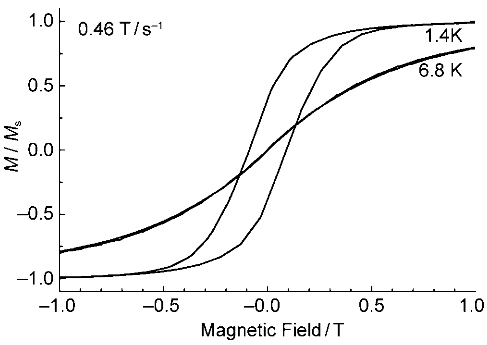

Figure 3. Normalized magnetization, M/M_s, versus DC applied field for a polycrystalline sample of **1**, obtained at the indicated temperatures with a fixed sweep rate of 0.46 $\mathrm{T\,s^{-1}}$.

0.01 $\mathrm{T\,s^{-1}}$). Taken together, these data confirm that at low temperatures, **1** is a SMM.

The temperature-dependent Mössbauer spectra of powdered samples of **1** show composite quadrupole-split doublets from 280 to 160 K, which appear as two broad and asymmetric absorptions (Supporting Information, Figure S7). Dipolar splitting owing to internal magnetic fields was not observed for temperatures above 20 K. At 20 K, the spectrum consists of a doublet and a broad absorption peak at the center of the spectrum, which is typical for a relaxation at intermediate rates (Supporting Information, Figure S8). At 3 K, a well-defined magnetic spectrum with the characteristic six absorption lines is observed (Figure 4), which indicates that the spin relaxation has crossed from fast to slow on the Mössbauer timescale. The spectrum was fitted with a sextet (parameters listed in the Supporting Information, Table S2). The lines are weakly broadened, which is probably due to slight differences in the local symmetries and hyperfine internal magnetic fields on the four Fe^{III} ions.

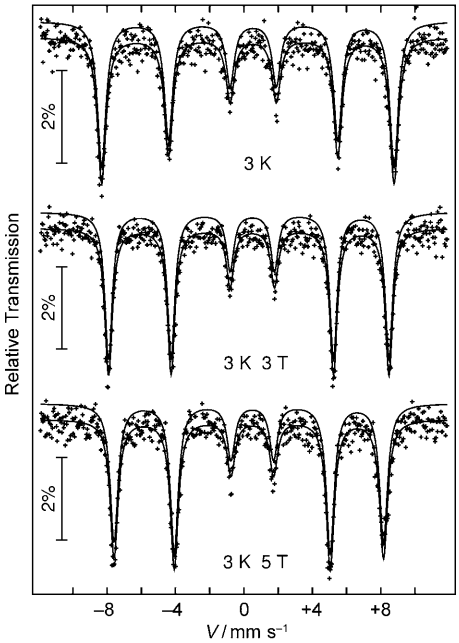

Figure 4. The ^{57}Fe Mössbauer spectra for **1** at 3 K and zero field, and at 3 K with applied magnetic fields of 3 T and 5 T oriented perpendicular to the gamma ray.

From the fitting parameters, the angle ϕ between the orientations of the internal magnetic field B_{int} and the main electric field gradient principal axis (V_{zz}) can be found according to the formula $\varepsilon = {}^1\!/_2 \Delta E_Q(3\cos^2\phi - 1)$, where ε is the quadrupole shift observed in the magnetically ordered spectra and ΔE_Q the quadrupole splitting values from the disordered (paramagnetic) spectra. Given that ΔE_Q approaches constant values[6] at low temperatures, the average value of ϕ could be calculated to be about 87.5°.

For a polycrystalline sample, the type of magnetic ordering can be determined from measurements in external magnetic fields. For a ferromagnetic material, an alignment of the magnetic moments along the external field B_{ext} with a concomitant rotation of the internal field is expected so as to reduce the nuclear hyperfine field. As seen from the Mössbauer spectra at 3 K in external fields of 3 and 5 T (Figure 4), an additional magnetic splitting does not occur, but the positions of the peaks shift slightly inwards, that is, the hyperfine field is slightly reduced (see also Supporting Information, Table S2). The direction of the Fe^{III} electronic spins with respect to the applied field can also be inferred from the relative intensity of the second and fifth lines with respect to the other lines, as this ratio is determined by the angle θ between $B_{\text{eff}} = B_{\text{int}} + B_{\text{ext}}$ and the incoming gamma rays. Here the intensities of the middle lines exhibit minor changes, which correspond to a slight increase of θ from 61.2 to 63.8°; that is, the effective field rotates only slightly towards the direction of the applied field (i.e., perpendicular to the incident gamma rays). All of these observations demonstrate a clear resistance of the Fe^{III} magnetic moments to tilt towards the applied magnetic field. It seems that for **1** a field larger than 5 T is necessary to achieve a significant alignment of the electronic spins of the Fe^{III} ions. Such behavior is expected for a system dominated by magnetic anisotropy. For the Dy^{III} ions, the applied fields of several Tesla are certainly too weak to turn their moments significantly away from their local quantization axes, which suggests that the observed stiffness of the Fe^{III} moments originates in fact from the interaction of Fe^{III} with Dy^{III} ions in the molecule. Given that the high-spin Fe^{III} is a relatively isotropic ion, this suggests that the major contribution to the magnetic anisotropy is induced in **1** by the Dy^{III} ions, and that these also dictate the easy axis of the molecular magnetization.

In conclusion, a combined magnetic and Mössbauer study on the first example of a ferromagnetically coupled Fe–Dy coordination cluster has been performed. Using these two complementary techniques enables us to obtain a more complete picture of the magnetic properties of such compounds. The presence of anisotropy slows down considerably the relaxation of magnetization, which results in SMM behavior. The energy barrier for reversal of magnetization assessed from AC susceptibility data Δ is 30.5 K and the corresponding relaxation time is $\tau_0 = 2.0 \times 10^{-9}$ s. Further studies on analogues involving diamagnetic, isotropic, and other anisotropic lanthanides are in progress.

Experimental Section

1: A solution of triethanolamine (0.111 g, 0.74 mmol) in MeCN (20 mL) was added dropwise over 20 minutes to a stirred solution of $DyCl_3 \cdot 6H_2O$ (0.07 g, 0.25 mmol), $FeCl_3$ (0.08 g, 0.50 mmol), and NaN_3 (0.034 g, 0.50 mmol) in MeOH (10 mL). The mixture was heated under reflux for one hour, cooled to room temperature, and then allowed to stand undisturbed in a sealed vial. Orange needles of **1** were obtained after 3 days in 42 % yield. The crystals were collected by filtration and washed with MeCN. C,H,N analysis (%) calcd for $Dy_4Fe_4C_{48}H_{108}N_{32}O_{26}$ (corresponds to loss of all acetonitrile solvent molecules): C 23.62, H 4.54, N 18.36; found: C 23.77, H 4.53, N 17.88. IR (KBr): $\tilde{\nu} = 3414$ (w), 2075 (s), 2037 (w), 1630 (s), 1419 (m), 1384 (s), 1285 (w), 1063 (m), 1025 (w), 897 (s), 743 (w), 645(w), 548 (w), 472 cm^{-1} (w).

Crystal structure of **1**: Data were measured at 100 K using a Bruker SMART Apex diffractometer with graphite-monochromated $Mo_{K\alpha}$ radiation. Structure solved using direct methods and refined using full-matrix least-squares with the SHELXTL program suite.[7] $C_{56}H_{120}Dy_4Fe_4N_{36}O_{26}$ (2587.28 $g\,mol^{-1}$); monoclinic, $P2_1/n$, $a = 23.9061(9)$, $b = 14.7796(6)$, $c = 26.4396(10)$ Å, $\beta = 97.121(1)°$, $V = 9269.7(6)$ Å^3, $T = 100$ K, $Z = 4$, $\rho_c = 1.854\ g\,cm^{-3}$, $F(000) = 5136$, $\mu(\text{Mo-}K_\alpha) = 3.876\ mm^{-1}$. 63 408 reflections measured, 21 040 unique ($R_{int} = 0.0385$), refinement (1202 parameters) to $wR_2 = 0.0975$, $S = 1.032$ (all data), $R_1 = 0.0390$ (17 543 data with $I > 2\sigma(I)$, largest final difference peak/hole $+2.54/-1.24$ e Å^{-3}. Three metal atoms, Fe(2), Dy(2), and Fe(3), are slightly disordered and were refined as pairs of atoms with occupancies 87.7 % and 12.3 %. No attempt was made to refine the ligand atoms of the minor component. CCDC 767230 contains the supplementary crystallographic data for this paper. These data can be obtained free of charge from The Cambridge Crystallographic Data Centre via www.ccdc.cam.ac.uk/data_request/cif.

Received: February 23, 2010

Keywords: iron · lanthanides · magnetic properties · Mössbauer spectroscopy · single-molecule magnets

---

[1] a) G. Abbas, Y. Lan, V. Mereacre, W. Wernsdorfer, R. Clérac, G. Buth, M. T. Sougrati, F. Grandjean, G. J. Long, C. E. Anson, A. K. Powell, *Inorg. Chem.* **2009**, *48*, 9345, and references therein; b) M. N. Akhtar, V. Mereacre, Gh. Novitchi, J.-P. Tucheagues, C. E. Anson, A. K. Powell, *Chem. Eur. J.* **2009**, *15*, 7278.

[2] D. Gatteschi, *Adv. Mater.* **1994**, *6*, 635, and references therein.

[3] O. Kahn, *Molecular Magnetism*, VCH, New York, **1993**.

[4] O. Kahn, *Angew. Chem.* **1985**, *97*, 837; *Angew. Chem. Int. Ed. Engl.* **1985**, *24*, 834.

[5] a) C. Benelli, D. Gatteschi, *Chem. Rev.* **2002**, *102*, 2369, and references therein; b) R. Sessoli, A. K. Powell, *Coord. Chem. Rev.* **2009**, *253*, 2328, and references therein.

[6] G. J. Long, F. Grandjean *in Supermagnets, Hard Magnetic Materials* (Eds.: G. J. Long, F. Grandjean), Kluwer Academic, Dordrecht, **1991**, p. 355.

[7] G. M. Sheldrick, SHELXTL 6.12, Bruker AXS Inc., 6300 Enterprise Lane, Madison, WI 53719–1173, USA **2003**.